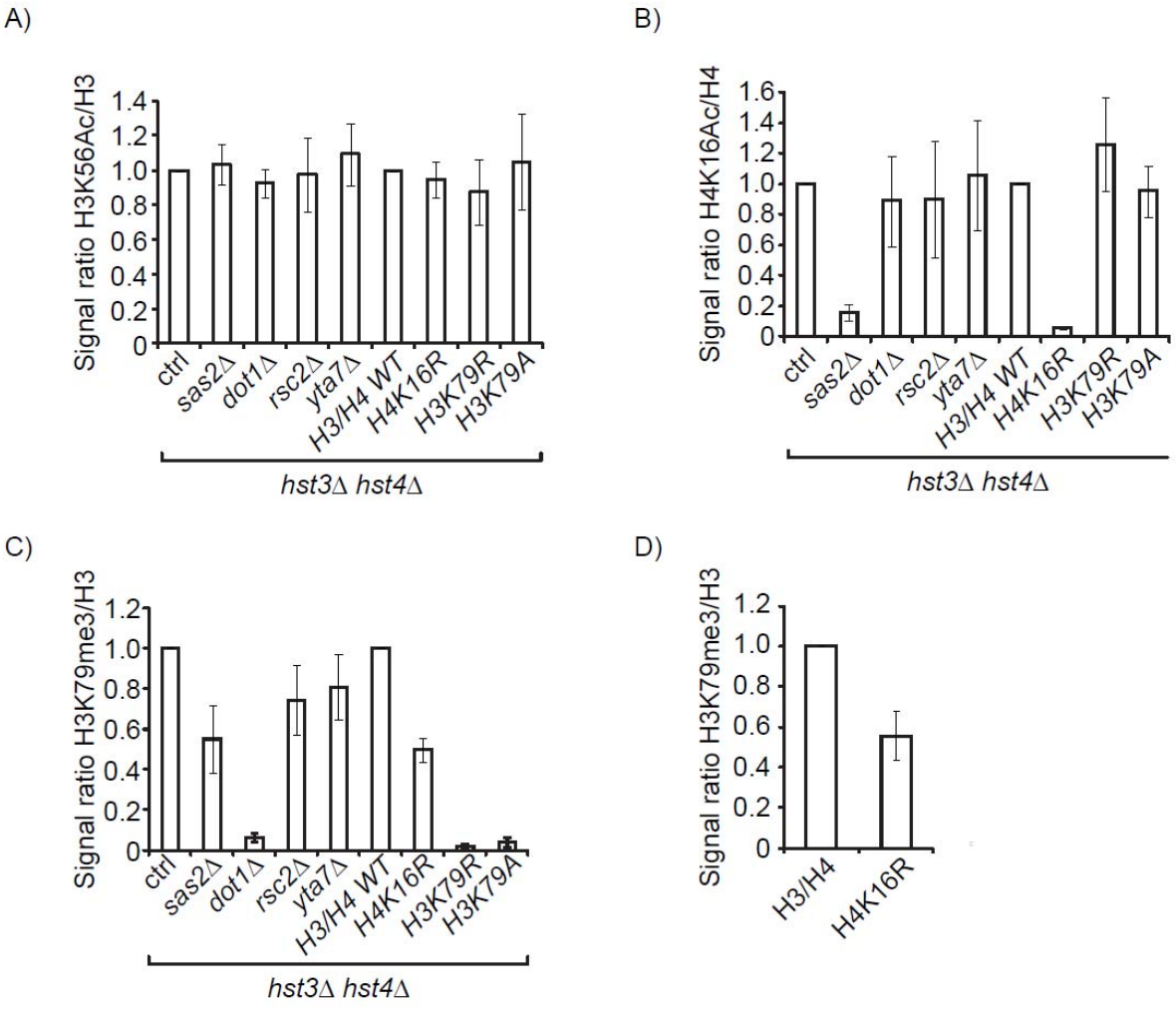

Figure S1 Densitometry analysis of immunoblots shown in Figure 4D and E**.** A-C) Immunoblot images from Figure 4D were analyzed by densitometry. Error bars represent the standard error of the mean of between 3 to 12 independent loadings of each sample. D) H3K79me3 immunoblot images from Figure 4E were analyzed by densitometry. Average values relative to the control signal derived from total histone H3 are shown and error bars indicate the standard error of the mean (from 4 independent loading of each sample).

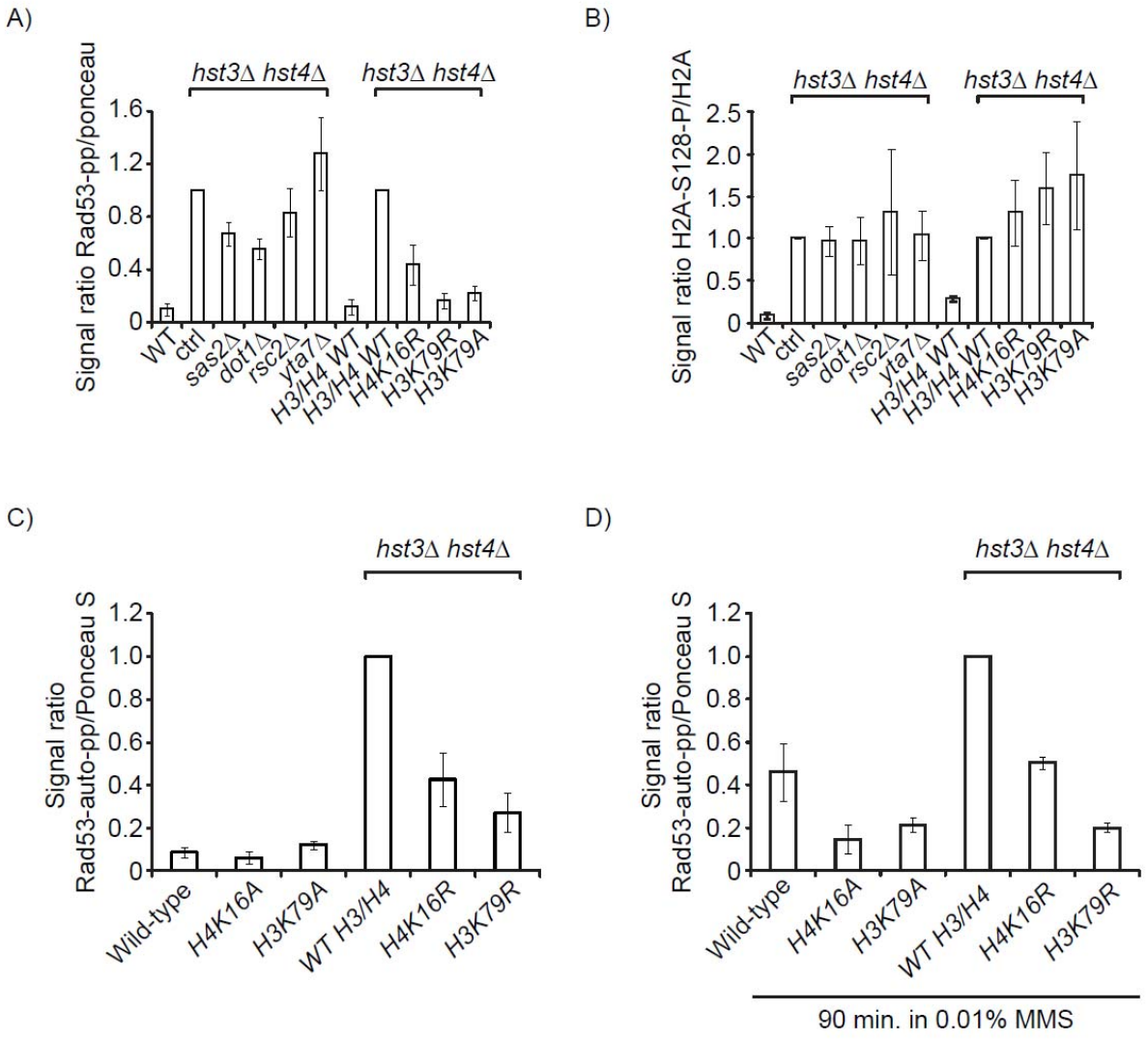

Figure S2 Densitometry analysis of immunoblots and Rad53 autophosphorylation assays shown in Figure 6B and 6C. A-B) Immunoblot or Rad53 autophosphorylation images from Figure 6B were analyzed by densitometry. Average signals relative to that observed in an isogenic *hst3*Δ *hst4*Δ strain are shown and error bars indicate the standard error of the mean (from at least 3 independent loadings of each sample).

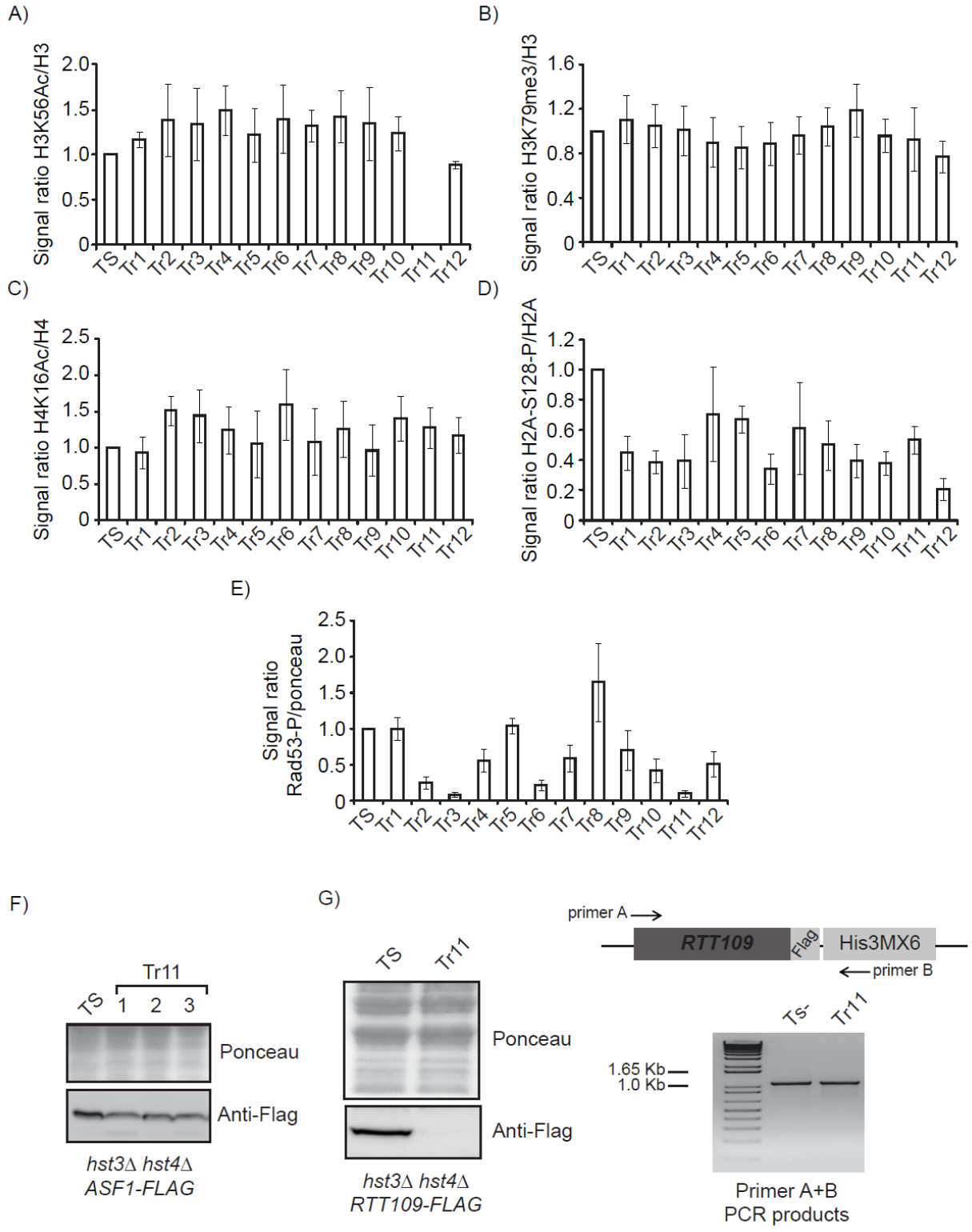
A)
Signal ratio H3K56Ac/H3
B)
Signal ratio H3K79me3/H3
C)
Signal ratio H4K16Ac/H4
D)
Signal ratio H2A-S128-P/H2A
E)
Signal ratio Rad53-P/ponceau
TS Tr1 Tr2 Tr3 Tr4 Tr5 Tr6 Tr7 Tr8 Tr9 Tr10 Tr11 Tr12
F)
Tr11
TS 1 2 3
Ponceau
Anti-Flag
hst3Δ hst4Δ
ASF1-FLAG
G)
TS Tr11
Ponceau
Anti-Flag
hst3Δ hst4Δ
RTT109-FLAG
primer A
RTT109
Flag
His3MX6
primer B
Ts- Tr11
1.65 Kb
1.0 Kb
Primer A+B
PCR products

Figure S3

Figure S3 Densitometry analysis of immunoblots and Rad53 autophosphorylation assays shown in Figure 7B. A-E) Immunoblots and Rad53 autophosphorylation images from figure 7B were analyzed by densitometry. The y-axes represent ratio of the signals obtained in each thermo-resistant strain (Tr) relative to the signal observed in the parental *hst3*Δ *hst4*Δ TS strain. Error bars indicate the standard error of the mean (at least 3 independent loading of each sample). F) Asf1 was epitope-tagged in the *Tr11* thermo-resistant spontaneous suppressor derived from *hst3*Δ *hst4*Δ Ts- mutant cells. Three independent clones derived from tagging Asf1 in the Tr11 strain were selected. Immunoblots of whole-cell lysates were probed to detect Asf1-Flag. Ponceau S staining is shown as loading control. G) The Rtt109-Flag protein is not detectable in the *Tr11* spontaneous suppressor of *hst3Δ hst4Δ* that lack H3K56Ac. Rtt109-Flag was detected by immunoblotting in whole-cell lysates of exponentially growing cells probed with a Flag antibody. (Right panel) Location of PCR primers used to ensure that DNA integration correctly resulted in an *RTT109-Flag* gene and PCR results showing that the *RTT109-Flag* gene is present in each of the strains analyzed for Rtt109-Flag protein expression in the left panel.

File S1

Supplementary Material and Methods

Histone purification, derivatization and mass spectrometry: Core histones were purified from yeast strains as previously described (GUILLEMETTE *et al.* 2011). Intact core histones were fractionated using an Agilent 1100 HPLC system equipped with a micro-fraction collector. Histone separations were performed using a ZORBAX 300SB-C8 column (5 µm, 300Å), 150×2.1 mm i.d. (Agilent Technologies), with a solvent system consisting of 0.1% trifluoroacetic acid (TFA) in water (v/v) (solvent A) and 0.1% TFA in acetonitrile (v/v) (solvent B). Gradient elution was performed from 5–90% B in 60 minutes at 150 µl/min. Fractions were collected in a 96-well plate at a rate of one fraction per minute. The fractions containing histone H3 were pooled and dried in a Speed-Vac concentrator. The dried samples were then subjected to propionylation to prevent internal cleavage of tryptic peptides lacking H3K56 acetylation or H3 peptides containing K79 that was either non-methylated or mono-methylated. Derivatization of intact histone H3 was conducted by adding a freshly prepared emulsion composed of 2:1 (v/v) water: propionic anhydride (Sigma), and vortexing for 1 h at room temperature. After the propionylation, samples were dried a second time, resuspended in 0.1 M ammonium bicarbonate, and digested overnight at 37°C using sequencing grade modified trypsin (Promega). The tryptic digests were dried to completion and resuspended in 0.2% formic acid in water (v/v) prior to mass spectrometry (MS) analysis. MS data were acquired in duplicate on a Q Exactive Plus mass spectrometer coupled to an EASY nLC II system (Thermo scientific). Peptides were first desalted on a Jupiter C18 (3-mm particles, Phenomenex) trap column (4-mm length, 360 mm i.d.) for 5 min at 10 µl/min, prior to their elution onto a C18 analytical column (18-cm length, 150 mm i.d.). A linear gradient from 5 to 60% acetonitrile (containing 0.2% formic acid) at 600 nl/min over 90 min was used for peptide elution. The MS instrument was operated in positive ion mode, and capillary voltage of 1.6 kV. MS scans were acquired in the Orbitrap analyzer over the range of 300 – 1500 *m/z* at a resolution of 70,000 and automatic gain control target value of 1.0×10^6. An inclusion list containing *m/z*, charge state and collision energy (CE) values of H3 peptides was used to trigger MS/MS acquisition. Every precursor ion found in the inclusion list was automatically selected for fragmentation in the HCD cell at a normalized CE setting of 27. The fragments were analyzed in the Orbitrap at a resolution of 35,000 and a target value of 5.5×10^5. The dynamic exclusion setting was disabled in order to acquire multiple MS/MS spectra per peptide. The relative abundance of peptides containing acetylated H3K56 or mono-, di- and tri-methylated H3K79 or their propionylated counterparts (corresponding to peptides that were not modified at K56 or K79 *in vivo*) was manually calculated from base peak intensities of extracted ion chromatograms.

H3K79me0, me1, me2 and me3: The percentages listed in Table 5 were calculated as follows. The relative abundance of H3 molecules lacking H3K79 methylation (K79me0) *in vivo* (expressed as percentage of all forms of the peptide containing K79),

was calculated as the abundance of the K79me0+pr peptide divided by the total abundance of the K79me0+pr, K79me1+pr, K79me2 and K79me3 peptides (where "pr" indicates *in vitro* propionylation). The same approach was employed to calculate the relative abundance of peptides containing H3K79me1, H3K79me2 and H3K79me3. *In vitro* propionylation can only occur on histone molecules that are non-methylated or mono-methylated *in vivo*; H3 molecules di- or tri-methylated *in vivo* cannot be propionylated. Hence, the percentages listed in Table 5 cannot be equated to stoichiometries because, after *in vitro* propionylation, the peptides with various degrees of methylation are chemically heterogeneous and, as a result, are not necessarily detected with the same efficiency (due to issues such as differences in charge and hydrophobicity affecting recovery from reversed phase HPLC and ionization/detection in the mass spectromer)(LIN *et al.* 2014).

H3K56ac stoichiometry: Because there is only one very abundant modification within the peptide containing K56, the percentages listed in Table 5 reflect stoichiometries of K56ac that were calculated as mentioned below. After *in vitro* propionylation, only two abundant tryptic peptides that differ by only one methylene group were detected: peptides derived from H3 molecules that lacked K56 acetylation *in vivo* (K56pr) and peptides that contained K56 acetylation *in vivo* (K56ac). Hence, the stoichiometry of H3K56 acetylation in each strain can be simply calculated as the abundance of the K56ac peptide divided by the total abundance of the K56ac and K56pr peptides. To ensure that K56ac stoichiometries were as accurate as possible, we also conducted two types of controls for the derivatization step. The first control was to ensure that *in vitro* propionylation proceeded with high efficiency. Inefficient propionylation of lysines that are not acetylated *in vivo* leads to overestimation of the stoichiometry of acetylation because peptides lacking lysine modification are cleaved by trypsin. The peptide that we monitored to determine the efficiency of propionylation was 57-STELLIR-63, which is generated by trypsin cleavage after a non-propionylated K56. Under our conditions, we estimated that a single round of propionylation led to an efficiency of H3K56 derivatization of 97.5%.

Second, it has been reported that, under certain conditions (*e.g.* multiple rounds of propionylation), propionylation can result in undesirable side reactions, such as O-propionylation of serine side chains (DROGARIS *et al.* 2008; LIAO *et al.* 2013). It is important to minimize these side reactions because peptides containing those modifications are chemically different from those containing only K56ac or K56pr and, therefore, difficult to take into account in calculations of acetylation stoichiometries. Under our conditions, we found that S57 propionylation occurred in roughly 6% of H3 moecules. Propionylation of H3-T58 was not detected. Based on this, we feel confident that undesirable H3-S57 or H3-T58 propionylation did not adversely affect our ability to determine H3K56Ac stoichiometries.

Supplementary references

DROGARIS P., WURTELE H., MASUMOTO H., VERREAULT A., THIBAULT P., 2008 Comprehensive profiling of histone modifications using a label-free approach and its applications in determining structure-function relationships. Anal. Chem. **80**: 6698–6707.

GUILLEMETTE B., DROGARIS P., LIN H.-H. S., ARMSTRONG H., HIRAGAMI-HAMADA K., IMHOF A., BONNEIL E., THIBAULT P., VERREAULT A., FESTENSTEIN R. J., 2011 H3 lysine 4 is acetylated at active gene promoters and is regulated by H3 lysine 4 methylation. PLoS Genet. **7**: e1001354.

LIAO R., WU H., DENG H., YU Y., HU M., ZHAI H., YANG P., ZHOU S., YI W., 2013 Specific and efficient N-propionylation of histones with propionic acid N-hydroxysuccinimide ester for histone marks characterization by LC-MS. Anal. Chem. **85**: 2253–2259.

LIN S., WEIN S., GONZALES-COPE M., OTTE G. L., YUAN Z.-F., AFJEHI-SADAT L., MAILE T., BERGER S. L., RUSH J., LILL J. R., ARNOTT D., GARCIA B. A., 2014 Stable-isotope-labeled histone peptide library for histone post-translational modification and variant quantification by mass spectrometry. Mol. Cell. Proteomics MCP **13**: 2450–2466.